https://doi.org/10.5194/egusphere-2026-1582
Preprint. Discussion started: 26 March 2026

Methane dynamics along the salinity gradient of the Scheldt estuary

Annalisa Delre[1], Thomas Röckmann[2], David J. Bonell Fontas[2], Julia C. Engelmann[1], Helge Niemann[1,3]

[1]Department of Marine Microbiology & Biogeochemistry, Royal Netherlands Institute for Sea Research (NIOZ), Texel, the Netherlands
[2]Institute for Marine and Atmospheric Research Utrecht (IMAU), Utrecht University, Utrecht, the Netherlands
[3]Department of Earth Sciences, Utrecht University, Utrecht, the Netherlands

Correspondence to: Annalisa Delre (annalisa.delre@nioz.nl)

Abstract. Estuaries are important natural sources of methane (CH_4) to the atmosphere. These transitional aquatic systems connect freshwater, brackish and fully marine environments. The pronounced salinity gradient, characteristic of estuaries, impose particular challenges to microbes and influence the biogeochemical processes they mediate. Salinity changes can inhibit methanotrophic activity. Here we analysed methane dynamics and microbial communities in the estuary of the Scheldt River, which flows through northern France, western Belgium, and the southwestern Netherlands, and finally discharges into the North Sea. During a research cruise conducted in June 2022 from the river mouth to Antwerp, water samples were collected at ten stations along the estuarine salinity gradient. We investigated water column CH_4 inventory and stable carbon isotope dynamics, together with methane oxidation rates. Elevated CH_4 concentrations of up to 110 nM with associated $\delta^{13}C$ -values of about −46‰ were found in the freshwater zone of the upper estuary (in the area of the city of Antwerp). Rather than a gradual decrease in CH_4 towards the North Sea, we observed a second maximum of 180 nM in the marine zone, with a contrasting isotopic composition of -66‰ indicating distinct methanogenic pathways and/or substrates in the estuary. Methane oxidation rates showed no clear relationship with the salinity gradient. In contrast, the composition of the methanotrophic community shifted markedly along the estuary and the salinity gradient, with *Methyloparacoccus* and *Crenothrix* prevailing in the freshwater zone *Methyloceanibacter* and *PLTB-vmat-59* dominating in the mixing and marine zones. Our results thus demonstrate that the salinity gradient is not the primary control on estuarine methane oxidation capacity but the community composition of the methane oxidizing bacteria (MOB). In sediments, the MOB community composition mirrored the patterns observed in the overlying water column, indicating that estuarine sediments represent both a key habitat and an important recruitment source sustaining methanotrophic communities in the water column. Despite an active microbial filter, methane oxidation accounted for only a minor fraction of the estuaries' CH_4 budget. Most methane (about 98%) was lost through advection and diffusive fluxes to the atmosphere, while a smaller fraction was exported to the North Sea, contributing to sustained methane supersaturation in coastal waters.

Keywords Salinity gradient · Methane budget · Stable isotopes · Methane oxidation · MOB community

https://doi.org/10.5194/egusphere-2026-1582
Preprint. Discussion started: 26 March 2026

1 Introduction

Methane (CH_4) is the second most important anthropogenic greenhouse gas after carbon dioxide (CO_2, IPCC, 2021). On a molecular basis, atmospheric CH_4 has a stronger impact on climate than CO_2, which is reflected by its 32-fold higher global warming potential (GWP) relative to CO_2 on a 100 year time horizon (Etminan et al., 2016). Moreover, CH_4 has a relatively short atmospheric lifetime of ~10 years (Canadell et al., 2021). Atmospheric CH_4 concentrations have been rising since industrialisation, reaching 1930 ppb in 2025 (Lan et al., 2025). This increase is largely driven by human activity, especially agriculture, fossil fuel extraction and use, waste disposal and land use change (Woodward et al., 2010, Ciais et al., 2013; Canadell et al., 2021, Fluet-Chouinard et al., 2023). However, global change-related warming and eutrophication were discussed to potentially cause elevated CH_4 fluxes from inland waters and the coastal ocean in the future. Coastal environments are extremely diverse encompassing shallow shelf seas as well as vegetated areas such as mangroves, salt marshes, and seagrass meadows, but also tidal flats and estuaries (Rosentreter et al., 2023).

A recent data-driven synthesis estimated that global estuaries - including tidal systems, deltas, lagoons, and fjords - emit ~0.25 (0.07–0.46) Tg CH_4 yr^{-1} (Rosentreter et al., 2023). As for most natural sources of atmospheric CH_4, estimates of CH_4 emissions from estuaries also remains highly uncertain due to pronounced spatial and temporal variability and limited observational coverage. The distribution of CH_4 input to estuaries is shaped by interacting processes, including upriver inputs, microbial production in the estuarine riverbed and inputs from industries (Scranton & McShane, 1991; Middelburg et al., 2002; Abril & Borges, 2004; Brown & Bass., 2022). Major removal pathways for dissolved CH_4 include river water release to the open sea, emissions to the atmosphere and microbial oxidation within the water column. The latter is moderated by aerobic methane oxidizing bacteria (MOB; Knief, 2015), which convert CH_4 to CO_2 thereby retaining a potentially important fraction of CH_4 in the estuarine water column (Abril & Iversen, 2002; Jacques et al., 2021; Mao et al., 2022).

The known MOB comprise Gammaproteobacteria (type I and type X), Alphaproteobacteria (type II), Verrucomicrobia, and members of candidate division NC10 (Knief, 2015). Molecular identification commonly relies on the 16S rDNA and the *pmoA* genes (Tavormina et al., 2008), although these markers primarily target currently known methanotrophs and may overlook novel or phylogenetically divergent lineages (Knief, 2015).

Microbial methane oxidation rates are strongly influenced by environmental conditions, including CH_4 concentration (Jakobs et al., 2013; Mau et al., 2013; Gentz et al., 2014), temperature (Lofton et al., 2014), oxygen availability (Guérin & Abril, 2007), suspended particulate matter (Middelburg et al., 2002; Abril et al., 2007), light (Dumestre et al., 1999; Murase & Sugimoto, 2005), translocation of methanotrophs with currents and rising bubbles (Schmale et al., 2015; Steinle et al., 2015) and notably salinity (de Angelis & Scranton, 1993; de Groot et al., 2025). Salinity is particularly relevant in estuarine transition zones, where freshwater and marine water mix. Several studies have shown that increasing salinity in estuaries is associated with reduced methane oxidation rates (de Angelis & Scranton, 1993; Osudar et al., 2015; Sherry et al., 2016). Other studies showed that salinity changes seemed to have rather small effects on the activity of methanotrophs and it has been suggested that methanotrophic communities may have adapted to such variability (de Groot et al., 2023, 2025; Zhang et al., 2023).

https://doi.org/10.5194/egusphere-2026-1582
Preprint. Discussion started: 26 March 2026

Finally, aerobic oxidation preferentially removes isotopically light CH_4, causing progressive ^{13}C-enrichment of the residual CH_4 pool (Whiticar, 1999). Analyses of CH_4 stable isotope signatures ($\delta^{13}C–CH_4$ and $\delta D–CH_4$) have proven highly effective in identifying CH_4 sources and sinks across diverse environments (Jacques et al., 2021). For example, Sasakawa et al., (2008) demonstrated that sinking particles are the primary source of subsurface CH_4 supersaturation in the oxygenated open ocean, where extensive microbial oxidation within particle microenvironments strongly modifies the isotopic signature of the produced CH_4.

The aim of this study is to quantify the distribution, transformation, and fate of dissolved CH_4 in the Scheldt estuary by integrating CH_4 concentrations, flux measurements, stable isotope signatures, and microbial oxidation rates. Specifically, we seek to (i) assess the relative contributions of riverine input, sedimentary methanogenesis, atmospheric efflux, and export to the coastal ocean; to (ii) quantify the activity, abundance, and community composition of methane-oxidizing bacteria and to (iii) evaluate environmental controls on MOB community dynamics and activity.

2 Materials and methods

2.1 Study area

The Scheld estuary boarders Northwest Belgium (Flanders) and the southwestern part of the Netherlands. It is highly eutrophic due to larges inputs of nutrients (Struyf al., 2004), contains elevated levels of heavy metals (Perrot et al., 20023) as well as organic pollutants (Van der Ael et al., 2012, Groffen et al., 2025). The estuary extends from the North Sea at Vlissingen (km 0) to Ghent (km 160). Upriver, sluices limit the tidal wave in the Upper Scheldt. The longitudinal salinity profile of the Scheldt estuary is primarily controlled by river discharge, with the transition between fresh and salt water being particularly variable (Van Damme et al., 2005; Soetaert et al., 2006). The estuary's water column is vertically well mixed (except during peak discharges). The horizontal salinity gradient is highly sensitive to seasonal changes in river discharge and to tidal oscillation (Meire et al., 2005). Previous studies indicated that dissolved CH_4 in the estuary is very high and variable at various spatial and temporal scales (Middelburg et al., 2002; Jaques et al., 2021), CH_4 was typically elevated at upriver locations.

2.2 Sampling scheme

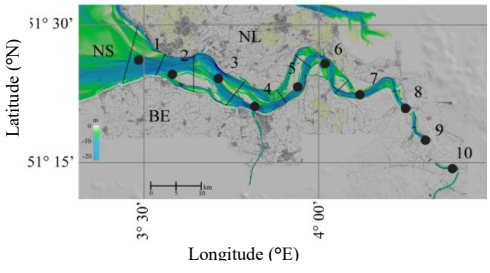

Figure 1. Study area with the locations of sampling stations (black dots) and station sections.

Water column and atmospheric sampling was conducted during a cruise with R/V Navicula in June 2022 along a gradient from almost fully marine (SW off Vlissingen, see Fig 1) to fully lacustrine conditions (Antwerp). We selected 10 stations that were approximately equidistant from each other. Water samples were taken with Niskin bottles from two different depths (de Groot et al., 2023): about 1 m above the estuaries' bed ("bottom") and 1 m below the water surface ("surface").

https://doi.org/10.5194/egusphere-2026-1582
Preprint. Discussion started: 26 March 2026

Samples were taken to analyze dissolved CH_4 and associated $\delta^{13}C$-values as well as MOx and associated MOB community structure. At four stations, we also collected sediments using a box corer (de Groot et al., 2023). Immediately upon recovery, the box corer was subsampled in triplicate with small pushcores (~18 cm sediment recovery). Surface sediments (0-5 cm) were collected in geobags (LDPE bags) and kept cold (4 °C) for incubation experiments. Finally, surface sediments were also sampled into 2 ml cryovials and kept at -80 ˚C for further molecular analysis.

2.3 Atmosphere measurements of CH_4 and water column atmosphere measurements

pCH_{4a} was measured with a Picarro G2301 gas concentration analyser on board. The instrument was directly connected to a floating chamber (0.08 m^3) and atmospheric values were recorded when the chamber was uplifted. We additionally collected gas samples in Tedlar Bags to ananlyse pCH_4 and associated $\delta^{13}C$-values as described previously (Jacques et al., 2021). The floating chambers were also used to measure the efflux of CH_4 from the sea surface/river surface. For this, the chamber was placed on the water surface with the rim of the chamber being kept submerged with attached weights. In this way, liberated CH_4 accumulates in the chamber. Accumulation was recorded online with the Picarro system and the efflux was calculated from the increase in CH_4 mixing ratio over time.

2.4 Dissolved methane concentrations and stable isotope ratios

Dissolved CH_4 concentrations were determined using a headspace (HS) technique (Green, 2005). In brief, 260 ml glass serum bottles were filled in triplicates from the Niskin bottle, closed with black-butyl rubber stoppers (Rubber B.V., the Netherlands) and crimped top-sealed. We then added 10 ml of N_2 (in exchange with sample water) to create a headspace and fixed the sample with 5 ml NaOH solution (25% w/v). CH_4 concentrations in the headspace were measured by gas chromatography with flame ionization detection (Thermo Scientific FOCUS GC) equipped with a Restek stainless steel column (HS-Q 80/100 SS GEN config, length 2 m, 2 mm ID, 1/8 OD) and using N_2 as a carrier gas (de Groot et al., 2023). From the same samples/bottles, the stable carbon isotope compositions was measured with a gas chromatography isotope ratio mass spectrometry system (GC-IRMS, Thermo Delta V, Thermo Fisher Scientific Inc., Germany) (Brass and Röckmann, 2010; Röckmann et al., 2016). All Isotopic values are represented in the delta notation ($\delta^{13}C$) against the Vienna Peedee belemnite (VPDB) standard. The GC and GC-IMRS systems were also used to measure CH_4 concentrations and stable carbon isotope composition during the incubation experiments (see below).

2.5 Methane oxidation rates (MOx)

MOx was determined through ex situ incubations with trace amounts of ^3H-labelled CH_4 as describe previously (Niemann et al., 2015). Aliquots from the Niskin bottle were filled in 20 ml glass vials in quadruplicates, sealed headspace free with grey-bromobutyl stoppers that are known to not hamper methanotrophic activity, and amended with10 µl $N_2/^3H$-CH_4 (4.5 kBq; American Rabiolabeled Chemicals, USA). Samples were incubated for 72 h at situ temperature in the dark. Activity of residual C^3H_4 and the product of methane oxidation (^3H_2O) were measured by liquid scintillation counting. First-order constant (k) was determined from the fractional turnover of the added tracer (Reeburgh, 2007):

https://doi.org/10.5194/egusphere-2026-1582
Preprint. Discussion started: 26 March 2026

$$k = \frac{^3H_2O}{^3H_2O + C^3H_4} \times \frac{1}{t} \qquad eq\ 1.1$$

Where t is incubation time in days. k was corrected for tracer turnover in killed controls (k_{KC}, fixed with 10ul $HgCl_2$ directly after sampling) and multiplied with methane concentrations [CH_4], to determine MOx:

$$MOx = (k - k_{KC}) \times [CH_4] \qquad eq\ 1.2$$

2.6 Stable isotope systematics of methanotrophy and methanogenesis

Apparent isotopic fractionation (ε) of the water column MOB community was determined from incubation experiments with water collected at 6 stations along the estuary. For this, surface water was collected in 2 l bottles from each station and triplicates of 99.5 ml estuarine water were filled into 260 ml crimp top vials in our home laboratories. After sealing the vials with red butyl rubber stoppers (Rubber B.V., the Netherlands), the remaining CH_4 from the estuary water was stripped out by percolating it with compressed air. We then established homogenous CH_4 concentrations in serum vials in the following way: we firstly created CH_4 saturated water by overlying 100 ml MilliQ with 100% CH_4 gas ($\delta^{13}C$ = -40‰) in a 260 ml crimp top vial which was left to equilibrate for 24h in a fridge. Then, 0.5 ml of CH_4 saturated water was injected into the incubation vials yielding a CH_4 concentration of 2.25 mM at the beginning of the incubation. Four additional bottles were prepared similarly, but 40 µl of $HgCl_2$ was added to stop biological activity (kill controls). The bottles were then incubated at 25°C in the dark and headspace measurements of CH_4 concentrations and stable carbon isotope composition were conducted every day for 3 days.

Ɛ-values associated with methane oxidation were determined from the fraction of the residual CH_4 and associated $\delta^{13}C$-values considering Rayleigh distillation processes for a closed system:

$$\delta = \delta_0 + \varepsilon \ln f \qquad eq\ 1.3$$

where δ is the $\delta^{13}C$ value of the residual CH_4, δ_o is the initial isotopic composition, and f is the fraction of CH_4 remaining.

Because the incubations were closed and no external CH_4 input occurred, the Rayleigh model appropriately describes the progressive ^{13}C enrichment of the remaining CH_4.

To determine the sedimentary source $\delta^{13}C$-CH_4 signature, 20ml sediment collected from box coring (see section 3.3) were mixed with 80 ml of local, CH_4-free estuary water. The bottles were then crimp top sealed with red butyl rubber stoppers and incubated at 25°C in the dark for 10 days. CH_4 concentrations and associated stable carbon isotope composition was measured every 2 days (see above).

2.7 Molecular identification of methanotrophic communities

DNA was extracted from particulate organic matter collected on filters (GF/F 47 mm, 0.3 µm nominal mesh size, Advantec MFS; pre-combusted at 450 °C for 4h) and sediment core tops using the DNeasy PowerSoil Pro Kit from Qiagen.

https://doi.org/10.5194/egusphere-2026-1582
Preprint. Discussion started: 26 March 2026

16S rRNA gene amplification was performed from biological triplicate with the universal SSU primer pair 515F-Y/806-R (515F: GTGYCAGCMGCCGCGGTAA, 806R: GGACTACNVGGGTWTCTAAT) targeting the V4 hypervariable regions. The forward and reverse primers were both barcoded with a unique 12 nucleotide Golay code. The PCR reaction mix contained 11.75 µl PCR grade water, 5 µl 5× Phusion HF buffer, 2 µl dNTPs (2.5 mM), 1 µl BSA (920 mg/ml), 0.25 µl (2 U/µl) Phusion polymerase, and 1.5 µl of each forward and reverse primer (10 µM) and 2 µl of DNA. PCR was performed in a thermocycler with the following program: 98°C for 30 s followed by 45 cycles of 98°C for 10 s 50°C for 20 s, 72°C for 30 s, with a final elongation of 72°C for 7 min; thereafter, samples were kept at 4°C.

PCR product concentrations were measured on a 4200 TapeStation - D1000 (Agilent, United States). Afterwards, they were pooled in equimolar amount and subjected to PCR purification using the QIAquick PCR purification kit (QIAGEN, United States) according to the manufacturer's instructions, followed by 1% gel electrophoresis. The band was visualized on a UV illuminator, excised from the gel and purified using the QIAquick gel extraction kit. Amplicon sequencing was carried out on an Illumina NextSeq 2000 sequencing platform (generating paired-end reads of length 2 × 300 nt) at USEQ (Utrecht University, the Netherlands).

The raw data were processed using the NIOZ in-house amplicon sequence analysis pipeline "Cascabel" (Abdala Asbun et al., 2020), according to the following specifications: Prior to AVS identification, reads were truncated to 270 bp and 200 bp for forward and reverse reads, respectively. AVS designation was done using DADA2 v.1.19.1. Chimeric sequences were identified based on consensus across samples and subsequently removed from the dataset. Similarly, singletons with an abundance lower than 2, were excluded from further analyses. Taxonomy weas assigned using DADA2's native implementation of the naïve Bayesian classifier method RDP by using the Silva v138.1 release (Quast et al., 2013) as reference database.

2.4 Abundance of methanotrophic bacteria assessed by quantitative PCR (qPCR)

For qPCR-based quantification of 16S rRNA gene copy numbers, the universal SSU primer pair 515F-Y/806R was used. The qPCR reaction mix contained 11.13 µl PCR grade water, 5 µl 5× Phusion HF buffer, 2 µl dNTPs (2.5 mM), 1 µl BSA (920 mg/ml), 0.625 µl EvaGreen 20× qPCR dye, 0.25 µl (2 U/µl) Phusion polymerase, and 1,5 µl of each forward and reverse primer (10 µM) and 2 µl of DNA template. A Bio-rad CFX Opus Real-Time PCR System was used to run the qPCRs. The cycling conditions for the qPCR reactions consisted of an initial 98°C for 30 s followed by 45 cycles of 98°C for 10 s 50°C for 20 s, 72°C for 30 s, with a final elongation of 72°C for 7 min; thereafter, samples were kept at 4°C.

2.5 Analysis of nutrients and dissolved carbon

Nutrients (PO_4^{3-}, NH_4^+, NO_3^-, NO_2^-) were analysed on a TRAACS Gas Segmented Continuous Flow Analyser (manufactured by Bran+Lubbe, now SEAL Analytical). All measurements were calibrated with standards diluted in low nutrient seawater (LNSW) in the salinity range of the samples (~35‰ to ensure that analysis remained within the same ionic strength; Murphy and Riley, 1962; Helder and de Vries, 1979; Grasshoff et al, 1983). *Dissolved Inorganic Carbon (DIC)* and *Dissolved Organic Carbon (DOC)* were analyzed as described in Delre et al. (2023). Briefly, for

https://doi.org/10.5194/egusphere-2026-1582
Preprint. Discussion started: 26 March 2026

DOC analyses, 30 ml was filtered using GF/F inline filters (nominal mesh size = 0.7 µm; pre-combusted at 450 °C for 4 h) mounted in steel cartridges, and the effluent was collected in pre-combusted glass vials (EPA), acidified with concentrated HCl to pH <2 and stored at 4 °C until analysis. DOC was measured with a Shimadzu TOC-V VCSH with ASI-V auto sampler after removal of inorganic carbon by vigorous sparging with oxygen. The water was then injected onto a combustion column packed with platinum-coated alumina beads at 720 °C. Non-purgeable organic carbon were combusted and converted to CO_2, which was then detected by a nondispersive infrared detector. For dissolved phase analysis, 5 ml of sample was taken immediately from the Niskin bottle for DIC analysis. This was also filtered over GF/F inline filters, and the effluent was collected headspace free in glass vials and analysed according to a method described previously (Stoll et al., 2001).

https://doi.org/10.5194/egusphere-2026-1582
Preprint. Discussion started: 26 March 2026

3 Results

3.1 Physicochemical parameters: water column and atmosphere

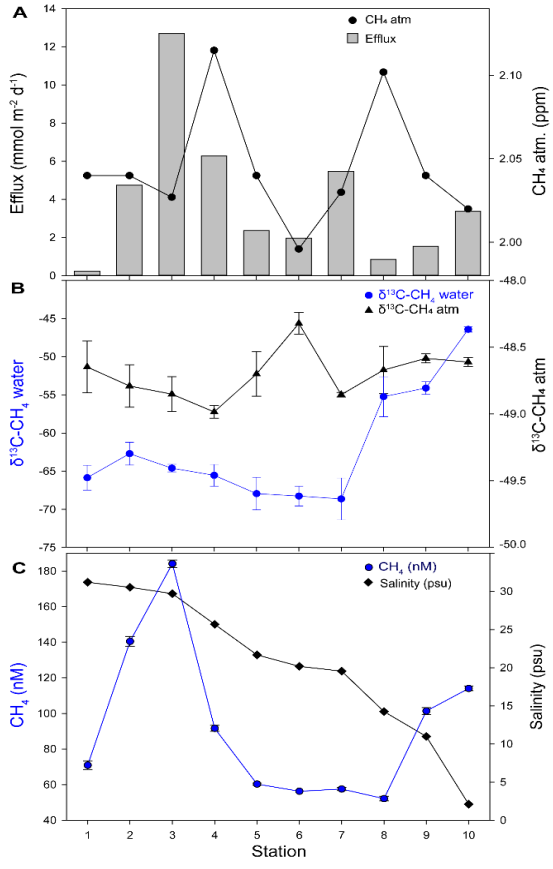

Figure 2 CH_4 dynamics in the Scheldt estuary. **A** Efflux of CH_4 from water surface to atmosphere and methane concentrations in the atmosphere. **B** $\delta^{13}C$-CH_4 (‰ vs VPDB) of CH_4 dissolved and in atmosphere **C** Water column methane concentrations and salinity.

Salinity & Temperature - Following a concave down distribution pattern, salinity decreased from 33psu at station 1 in the North Sea to brackish/freshwater values of 2 psu at station 10 in the city of Antwerp (Fig 2 C). Three groups of water samples were defined: freshwater zone (salinity: 2 psu; station 10), mixing/brackish zone (salinity: 11-20.2 psu; stations 6-9) and seawater zone (salinity: 21.7-31.2 psu; stations 1-5). Water column temperatures showed an increasing trend from the North Sea (17.9°C) to Antwerp (20.5°C; Fig A1 appendix A).

Methane - Water column CH_4 concentrations (Fig 2 C) were generally >50 nM and thus supersaturated with respect to the atmospheric equilibrium (see below). We detected two CH_4 maxima, one at stations 3 (180 nM) and a second at station 10 (110 nM), while CH_4 concentrations were more constant in the mixing zone between stations 5-8 (50-60 nM). In general, there were no notable differences in CH_4 concentrations in surface and bottom waters. Given the minimal differences between the two layers, only surface water concentrations are presented here. Stable carbon isotope ratios of dissolved CH_4 were generally low with values of -62‰ to -70‰ from station 1 – 7 but increased sharply to -46 ‰ at station 10.

Atmospheric CH_4 mixing ratios (Fig 2 A) showed small variations around 2 ppm with two peaks at station 4 and 8 (respectively 2.12 and 2.1 ppm). The associated δ^{13} C-CH_4 values (Fig 2 B) were generally around -48.8 and showed some smaller fluctuation, with the heaviest value at station 6 (-48.4‰). Atmospheric mixing ratios, surface water temperature and salinity levels translate to methane saturation levels of 2.9 nM at station 10 and 2.6 nM at station 1 (Wiesenburg & Guinasso, 1979). The entire estuary (CH_4 levels >50 nM at all sampling stations) was thus CH_4 supersaturated with respect to the atmospheric equilibrium and hence a source of CH_4 to the atmosphere. Also our floating chamber measurements revealed efflux of CH_4 from the river surface; this was highest at station 3, exceeding 12 mmol m^{-2} d^{-1}. Station 1 showed lowest CH_4 efflux with 0.2 mmol m^{-2} d^{-1} (Fig 2 A).

https://doi.org/10.5194/egusphere-2026-1582
Preprint. Discussion started: 26 March 2026

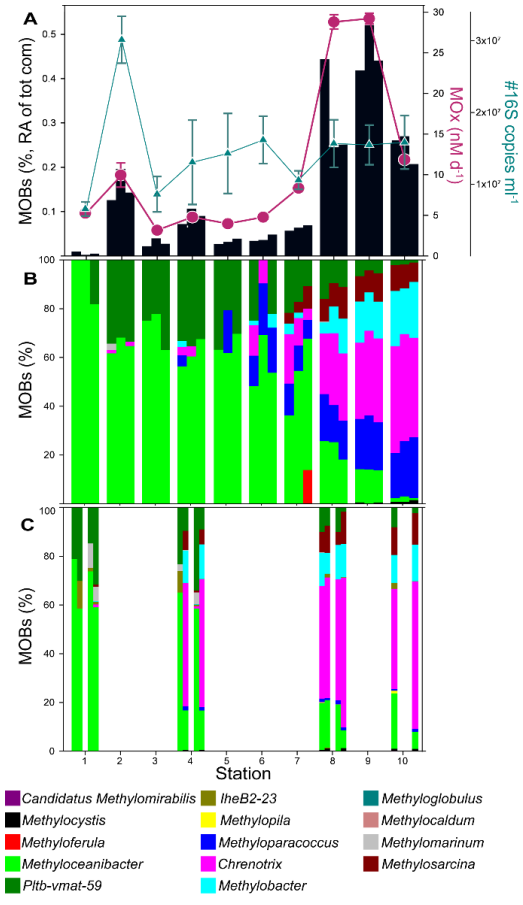

Figure 3 A Relative abundance of MOB in total microbial community (%), methane oxidation rates (MOx) and abundance of 16S gene copies. **B** MOB community composition (%) in the water column and (**C**) in the sediments. Station 10 has biological replicates but technical replicates are absents.

Nutrients, DIC, DOC - The distribution of NO_3^-, DIC and DOC concentration showed an apparent anticorelation when compared to salinity with lowest values in the North Sea at sation 1 (NO_3^-: 8 µM, DIC: 2330 µM, DOC: 161 µM), and highest values at station 10 (NO_3^-: 248 µM, DIC: 4087 µM, DOC: 488 µM; Fig A1 appendix A). Also NO_2^- and PO_4^{3-} followed this pattern with lowest concetrations at station 1 (NO_2^-: 0.4 µM, PO_4^{3-}: 0.2 µM). Yet, both nutrient types displayed a maximum at station 9 (NO_2^-: 1.25 µM, PO_4^{3-}: 4.8 µM). With regards to NH_4^+ concentration, two peaks were observed, one at station 3 (2 µM) and a second one at station 8 (4.2 µM), whereas values remained relatively constant in the mixing zone between stations 5-7 (0.4 µM).

3.2 Aerobic methane oxidation and methanotrophs

Methane oxidation rates (MOx) were always >5 nM d^{-1} and highest with values of > 29 nM d^{-1} in Antwerp (stations 8 and 9; Fig 3 A). We also found a second smaller MOx peak close to the river mouth (station 2) with 10 nM d^{-1}.

Mirroring the distribution of MOx, the relative abundance of water column MOB was highest at station 8 and 9 (accounting for ~0.5% of all ASVs), and a second maximum with a relative abundance of ~0.2% was encountered at station 2 (Fig 3 A). The number of 16S gene copies of the total community was generally ~1-2 × 10^7 copies ml^{-1} across most stations, with a peak at station 2 (3 × 10^7 copies ml^{-1}).

The distribution of MOB genera differed between stations in the North Sea and the mixing zone (stations 1-7) versus the freshwater zone (stations 8-10; Fig. 3 B). Waters from stations 1-7 were dominated by members of the potential MOB *Methyloceanibacter* and to a lesser degree by members of the *Pltb-vmat-59* group. Upriver at stations 8, 9 and 10, the contribution of *Methyloparacoccus* and *Chrenotrix* and to a lesser degree of *Methylobacter* and *Methylosarcina* became increasingly more pronounced, while the contribution of MOB dominant in the marine and mixing zone declined.

In sediments, MOB followed the same abundance pattern as observed in the water column, with a clear dominance of *Methyloceanibacter* at station 1, while upriver (stations 8 and 10), this trend shifted with *Crenothrix* emerging as the

https://doi.org/10.5194/egusphere-2026-1582
Preprint. Discussion started: 26 March 2026

most dominant genus (Fig 3 C). All MOB types detected in the water column were also present in sediments, however, we additionally detected minor abundances of *Candidatus Methylomirabilis*, *Methylocystits*, *Methyloferula*, *IheB2-23*, *Methylopila*, *Methyloglobulus*, *Methylocaldum* and *Methylomarinum*.

3.3 Isotope fractionation of methanotrophy and methanogenesis

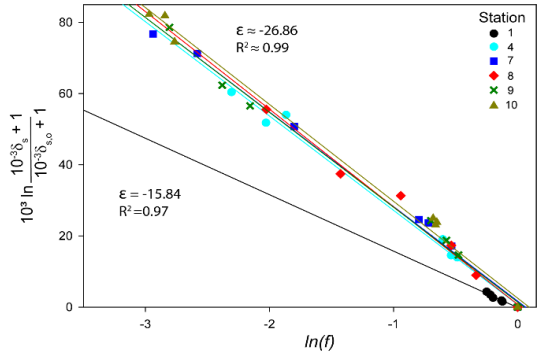

Figure 4 Rayleigh plot of CH_4 data from the incubation of water column methanotrophs. *f* is the fraction of methane remaining (the ratio between the CH_4 concentration at the beginning of the incubation and at the end). Linear regressions are plotted through the different stations, and the slope ε is equivalent to the isotope enrichment factor.

The amount of CH_4 in the headspace of closed incubations with river water decreased from 0.02 mmol to 0.002 mmol, while the corresponding $\delta^{13}C$– CH_4 values increased from −39‰ to approximately +20‰. Only incubations with water from Station 1 deviated from this pattern, only showing a minimal decrease in CH_4 concentrations, from 0.02 mmol at the start to 0.016 mmol at the end of the experiment. The $\delta^{13}C$–CH_4 signature at this sttion increased only slightly, from −34‰ to -32‰. The incubations were terminated after three days, by which time CH_4 concentrations were still sufficient for isotopic analysis. Apparent isotope fractionation (ε; Fig 4) was calculated using equation 1.3. Incubations with water from stations 2-10 showed comparable ε values of −26.9‰. Fully marine waters (station 1) showed a markedly lower ε value of −15.9‰).

We only found CH_4 production during incubations with riverbed sediments at two stations. Here, $\delta^{13}C$ measurements revealed CH_4 isotope signatures of −57.78‰ at Station 8 and −46.5‰ at Station 10.

4 Discussion

4.1 Methane distribution along the estuarine salinity gradient

CH_4 concentrations (52-184 nM) were consistently supersaturated relative to the atmospheric equilibrium (2.6-2.9 nM) throughout the estuary, directly showing that the river's surface waters are a source of CH_4 to the atmosphere. This observation aligns with previous publications from the Scheldt estuary reporting CH_4 concentrations in the range of 20-485 nM (Middelburg et al., 2002, Jaques et al., 2021). In fact, Jacques et al. (2021) observed highest CH_4 concentrations in the lower estuary near Vlissingen (95 nM; December 2015) and in the upper estuary near Antwerp (303 nM; November 2016). In our study, the highest concentration was detected near the lower estuary (station 3, 184 nM) and a second maximum near Antwerp (station 10, 114 nM). CH_4 concentrations of Scheldt waters are similar to other European estuaries typically showing supersaturation with respect to the atmospheric equilibrium, too (Stanley et al., 2022). Concentrations in the river Elbe, for example, were found to amount to 4-111 nM, while 5-273 nM were found in the river Thames and 4-559 nM in the river Gironde (Middelburg et al., 2002). In the Lena Delta, CH_4 concentrations were elevated nearshore and decreased with distance from the coast, ranging from 10 to 218 nM (Bussmann et al., 2017). Similar concentrations have also been documented in other European estuaries (Abril et al.,

https://doi.org/10.5194/egusphere-2026-1582
Preprint. Discussion started: 26 March 2026

2007; Upstill-Goddard et al., 2016; Matoušů et al., 2017; Stanley et al., 2022) suggesting similar types and strength of driving forces controlling CH_4 dynamics in these systems.

Our measurements show, moreover, that CH_4 concentrations did not exhibit a unidirectional trend along the estuary (i.e., a concentration gradient - increasing or decreasing – up- or downriver) and CH_4 concentrations did not follow the estuary's salinity gradient. This pattern has also been observed in the Elbe estuary (Matoušů et al., 2017) and other estuaries across Europe (Hackbusch et al., 2019; Upstill-Goddard and Barnes, 2016; Sánchez-Rodríguez et al., 2022). Even though some studies have reported decreasing CH_4 concentrations with increasing salinities (Rehder et al. 1998; Middelburg et al. 2002; Osudar et al. 2015), our data, together with previous results, challenge the paradigm that CH_4 and salinity are anticorrelated in estuaries. In contrast, our data rather suggest that local sources, including inputs from tributaries, sedimentary methanogenesis, and sinks such microbial oxidation and atmospheric efflux strongly modulate local CH_4 concentrations (de Groot et al., 2024). CH_4 dynamics in the Scheldt and potentially in other delta systems are thus not only governed by a two-endmember mixing comprising inflow from the upper river and export from the river mouth to the open sea with influences by tributaries and canals.

4.2 Methane oxidation rates in the water column

Methane oxidation rates showed a non-linear distribution along the estuary, with lower values in the mixing zone and distinct peaks both in saline and freshwater regions (Fig 3 A). Our observation is consistent with findings from the German Bight and the Elbe estuary, where microbial communities are frequently exposed to salinity—largely due to tidal influence. Along the salinity gradient of the Elbe, methane oxidation rates have been reported to range from 0.8 nM d^{-1} in the lower estuary to as high as about 5542 nM d^{-1}, particularly at the Hamburg harbour (Matoušů et al., 2017). In the German Bight, the highest methane oxidation rates (2.6 nM d^{-1}) were observed at coastal stations, whereas the lowest rates (0.4 nM d^{-1}) were found at the marine stations (Osudar et al., 2015). Several studies, nevertheless, observed a negative correlation between salinity and methane oxidations, highlighting salinity as the major factor controlling MOx by affecting the composition and activity of methanotrophic communities (Poffenbarger et al., 2011; Ho et al., 2018; Zhang et al., 2023). Specifically, salinity has been described to inhibit methane oxidation in freshwater systems (de Angelis and Scranton, 1993) and is often attributed to osmotic stress on freshwater MOB (Osudar et al., 2017). In contrast, we found relatively high rates of MOx (up to 5 nM d^{-1}) throughout the entire estuary, apparently independent of salinity. This consequently suggests that salinity changes are not necessarily inhibitory for methane oxidation. Similarly, more recent observations from the Wadden Sea (de Groot et al., 2023) and Svalbard (Steinle, et al., 2015) also showed that salinity changes seemed to have rather small effects on MOx and it has been suggested that methanotrophic communities may have adapted to such variabilities (de Groot et al., 2023, 2025; Zhang et al., 2023). Nevertheless, whether this pattern was related to an adaptation of specific MOB to variable salinity levels or to changes in the composition of the MOB community as a function of salinity variation was not investigated in previous studies.

https://doi.org/10.5194/egusphere-2026-1582
Preprint. Discussion started: 26 March 2026

4.3 Methanotroph community shifts along the salinity gradient

Methanotrophs were detected throughout the entire Scheldt estuary, both in the water column and in sediment samples. However, we observed a clear shift in community structure along the salinity gradient: *Crenothrix*, *Methylobacter*, *Methyloparacoccus* and *Methylosarcina* in the upper, fresh water part of the estuary were successively supplanted by *Methyloceanibacter* and *Pltb-vmat-59* in the middle, brackish water section, while the marine endmember of the estuary water column was dominated by *Methyloceanibacter*. These shifts are likely driven by the differential sensitivity of MOB groups to a range of salinities, which was discussed to shape community composition of MOB (Osudar et al., 2017, Zhang et al., 2023) and broader prokaryote community structure in estuarine water columns (Wu et al., 2024). *Crenotrix* is indeed typically detected in freshwater systems (Yang et al., 2022) and *Methyloceanibacter* in marine waters (Vekeman et al., 2016; de Groot et al., 2024, 2025). Members of the *Methylobacter*, *Methyloparacoccus* and *Methylosarcina* genera have previously been found in brackish, coastal zones such as mangroves (Das et al., 2024) and the Dutch Wadden Sea (de Groot et al., 2025), but also in fully marine systems, e.g. cold seep systems (Tavormina et al., 2008) and sediments (Tavormina et al., 2015). Pltb-vmat-59, on the other hand, has mostly been found in marine waters (de Groot et al., 2024) and was also found as a dominant group in incubation experiments with North Sea waters (de Groot et al., 2025). Our findings of these genera in the upper – mid estuary, but not the lower, marine dominated sections of the estuary suggests that these groups may contain strains that are specifically adapted to brackish/freshwater conditions.

Absolute microbial abundance determined by 16S copy numbers together with the relative contribution of MOB to the prokaryote community indicates that the overall abundance of MOB remained relatively constant across the freshwater-marine transition. Note that this is only a rough approximation as the frequency of 16S operons per genome can vary between 1 up to 15 (Klappenbach et al., 2001). However, despite the differential water column MOB community composition, overall MOx was not substantially affected by salinity (see previous section), but instead followed MOB abundances. This suggest that salinity may indeed exert a selection pressure on the composition of the MOB community but that system-level MOx is determined by the abundance of MOB rather than their identity. It needs to be stressed, however, that this may be different for other environments. In incubations experiments, de Groot et al., (2025), for example, found that salinity had only a week effect on MOB community composition. Other studies showed that elevated salinity often led to an immediate decrease in MOx in terrestrial/lacustrine systems (Ho et al., 2018; Zhang et al., 2023). Likewise, marine methanotrophs seem to function best at salinity levels of 20 psu (Osudar et al., 2017), while a sudden decrease in salinity can inhibit MOx (Hirayama et al., 2013; Tavormina et al., 2015).

Our data consequently show that salinity seemingly influence MOB community composition but not their overall activity, but that MOB abundance primarily governs overall MOx. Considering the current velocity of the Scheldt (~95 km d^{-1}, Meire et al., 2005), a typical doubling time of MOB (~9 days, Mayr et al., 2020) and the length of the estuary investigated here (87 km) it seems unlikely that shifts in MOB composition are primarily driven by growth within the water column. However, given the presence of similar methanotrophs in both sediments and overlying waters, it is more plausible that the sediment community acts as a reservoir supplying MOB to the water column. Shear forces exerted by the river current likely cause resuspension and thus mobilisation of sedimentary MOB. Similar to resuspension caused by tidal currents (de Groot et al., 2023) and bubbles peculating through sediments (Steinle et

https://doi.org/10.5194/egusphere-2026-1582
Preprint. Discussion started: 26 March 2026

al., 2015, Jordan et al., 2020, 2021), this could be a key driver in determining estuarine water column MOB communities in rivers.

4.4 Isotopic signature along the Scheldt estuary

The $^{13}C–CH_4$ signatures measured along the Scheldt estuary are consistent with a predominantly microbial methane source (Whiticar., 1999) and match the isotopic composition of newly produced methane in our sediment incubation experiments (Fig 4). Previous investigations, however, reported unusually heavy $\delta^{13}C–CH_4$ values of up to −25‰ in the upper Scheldt estuary (Jacques *et al.*, 2021), whereas our maximum $\delta^{13}C–CH_4$ value was -46 ‰. We cannot fully explain this discrepancy. Based on CH_4 concentration and isotopic composition, Jacques *et al.* (2021) estimated an ε-value for water column MOx of -12.8 ‰. Considering this and their CH_4 concentration and associated $\delta^{13}C$-values, they concluded that ~80% of the methane must have been oxidized by MOB to account for such enrichment. Our experimental measurements, in contrast, yielded MOx-related ε-values of ~-26.9‰.

Considering the highest CH_4 concentration and associated $\delta^{13}C$-value measured here (180 nM and -64.6‰; Fig 2 C, B), we re-calculated that about 50% of the CH_4 had been consumed to account for the observed isotope enrichment. However, these theoretical CH_4 consumption estimates are in stark contrast when compared to our CH_4 budget of the Scheldt estuary (see next section below). Our CH_4 budget combines ex situ MOx rate measurements and direct CH_4 efflux measurements and indicates that only ~1% of CH_4 was consumed in the water column. We cannot fully explain the discrepancy between CH_4 isotope dynamics and direct measurements of consumption. However, isotope signatures can integrate metabolic processes over larger spatial and temporal scales (Parnell et al., 2010). It seems hence likely that the observed signatures are inherited from riverine oxidation processes upstream of the city of Antwerp. Additionally, the CH_4 source isotopic composition might likely be variable along the river. This is also indicated by the change in the CH_4 $\delta^{13}C$-values, rapidly dropping from about -46‰ in the city of Antwerp to <-60‰ just downstream of the city (station 7). This spatial trend agrees with the overall pattern reported previously (Jacques et al., 2021; note that absolute isotopic values differed in the previous and our study). The observed shift suggests a transition from a relatively ^{13}C-enriched methanogenic substrate to a lighter one or, alternatively, a change in methanogen community composition and associated methanogenic pathways and/or isotope fractionation (Krzycki *et al.*, 1987; Whiticar, 1999; Gropp, 2022). Finally, MOx in the estuary might have been considerably higher during the sampling period of Jacques *et al.* (2021), leading to stronger enrichment of the residual CH_4 in ^{13}C (Whiticar, 1999; Jacques *et al.*, 2021).

4.5 Fluxes and budget

By applying an area-weighted extrapolation of CH_4 fluxes from the ten, roughly equidistant floating chamber stations we estimate a mean methane efflux to the atmosphere of approximately 4 mmol m^{-2} d^{-1} across the entire Scheldt estuary. This is well within the range of previous reports from other estuaries (Tab. 1).

https://doi.org/10.5194/egusphere-2026-1582
Preprint. Discussion started: 26 March 2026

Table 1. Efflux of methane in estuaries inside and outside Europe

River	Efflux (mmol m^{-2} d^{-1})	Reference
Danube	1.176 ± 1.464	Canning et al., 2021
Guadalquivir	0.12	Sanchez et al., 2022
Randers Fjord	0.02-0.4*	Abril and Iversen (2002)
Temmesjoki, Finland	1.6*	Silvennoinen et al. (2008)
Río San Pedro	0.08*	Ferrón et al. (2007)
Ria de Vigo	0.003*	Kitidis et al. (2007)
Tay	0.05*	
Tees	0.5*	
Tyne	1.3*	Upstill-Goddard and Barnes, 2016
Tamar	0.3*	
Forth	0.2*	
Humber	0.03*	
White Oak River estuary	17.1	Kelley et al., 1990
Yangtze estuary	0.003-0.4	Zhang et al., 2008
German Bight	0.003-0.277	Bussmann et al., 2021

* recalculated from annual averages

Per unit area, many estuaries thus emit >10-fold more CH_4 to the atmosphere when compared to fully marine coastal zones (Rosentreter et al., 2023). For example, methane efflux from the highly active seeps in the Belgium coastal zone were found to range between 0.001–0.4 mmol m^{-2} d^{-1} (Borges et al., 2016). Similarly, the highly active cold seeps at the Doggerbank in the North Sea were found to emit between 0.06 to 0.18 mmol m^{-2} d^{-1} (de Groot et al., 2024). In deeper continental shelf systems, CH_4 bubbles exchange gas with the adjacent water during their rise (Gentz et al., 2014; Leifer & Patro, 2002; McGinnis et al., 2006). For example, a pure methane bubble of ~5 mm diameter rising from 40 m water depth will have lost ~50 % of its methane content before breaking the surface (McGinnis et al., 2006). The dissolved CH_4 can then be removed through microbial oxidation and advective transport can translocate and further disperse the CH_4 (Abril & Iversen, 2002; von Deimling et al., 2011; James et al., 2016; de Groot et al., 2024). In contrast, in shallow systems such as estuaries and tidal flats, bubbles emitted from sediments may only exchange a minor fraction of their gas content during their ascent (de Groot et al., 2023; McGinnis et al., 2006). In addition, rivers are typically not stratified and characterized by turbulent mixing so that dissolved gases are rapidly exchanged with the atmosphere.

https://doi.org/10.5194/egusphere-2026-1582
Preprint. Discussion started: 26 March 2026

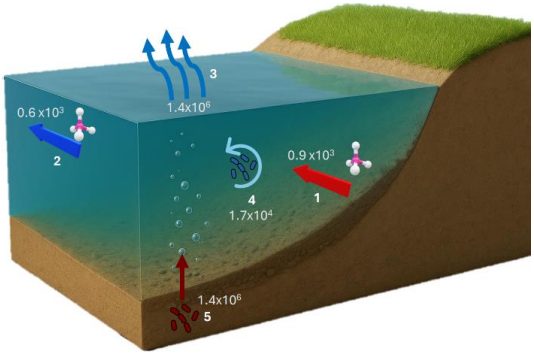

Figure 5 (Generated with AI) Methane budget for the Scheldt estuary (mol d^{-1}) is calculated based on the area between the 10 stations. **1** influx from Antwerp (into the estuary) **2** outflow into the North Sea **3** methane efflux **4** methane oxidation **5** methane liberation from the sediments

Towards a rough estimation of a CH_4 budget of the Scheld estuary, we integrated efflux data as determined from our floating chamber measurements, ex situ MOx measurements and methane concentration data as well as estimates of water volume and flow velocity (Fig 5, see also appendix A table A1). With respect to the volume flux of the river at Antwerp (100 m^3 s^{-1}, Waterinfo Vlaanderen) and the CH_4 concentration of 114 nM measured here (station 10), we estimate an input of CH_4 from upriver to the city of Antwerp (F_{in}) of 985 mol CH_4 d^{-1}, at least during the time period of our observations (Fig 5). Similarly, considering the river's discharge (110 $m^3 s^{-1}$, Rijkswaterstaat) and our measured CH_4 concentration of 71 nM (station 1), CH4 export into the North Sea (F_{out}) is ~674 mol CH_4 d^{-1}. Along the flow path, we divided the estuary between the measurement stations in equidistant sections (Fig 1). Considering areal CH_4 efflux measurements (0.2-12.7 mmol m^{-2} d^{-1}) and the surface areas of the sections (5-61 km^2), approximately 1.4 × 10^6 mol CH_4 d^{-1} are released to the atmosphere (J_{atm}). Similarly, our MOx (3.2-29.2 nM d^{-1}) measurements and the volume of each section (1.8 – 8.5 × 10^{11} m^3) translate to a total CH_4 consumption (MOx_{tot}) of ~1.7 × 10^4 mol CH_4 d^{-1}. Hence, considering all input and output terms for CH_4 as outlined above, the amount of CH_4 supplied to the estuary from sediment methanogenesis (MOg_{tot}) can be calculated as:

$$MOg_{tot} = J_{atm} + MOx_{tot} + F_{out} - F_{in} \qquad eq\ 1.4$$

We estimated that MOg_{tot} amounts to 1.4x10^6 mol CH_4 d^{-1}.

Overall, these results suggest that most of the methane in the Scheldt estuary is released to the atmosphere, while only a minor fraction is transported toward the adjacent coastal marine environment and consumed within the water column. Also, only a minor fraction of the estuary's methane originates from upriver, while most is produced in the estuary's sediments.

5 Summary and Conclusions

The Scheldt estuary is a transitional environment characterized by a pronounced salinity gradient that divides the system into three distinct zones, ranging from freshwater in the upper estuary to fully marine conditions near the estuarine mouth. Our study revealed substantial spatial variations in methane dynamics that are not directly related to the salinity gradient. Salinity appears to be an important selection factor for MOB. This suggests that estuarine sediments not only serve as a critical habitat for methanotrophic communities but also play a key role in sustaining and replenishing the MOB population in the overlying water column. Nevertheless, the MOx filter capacity in estuaries seems to be limited only retaining a minor fraction of CH_4, while most is released to the atmosphere. Furthermore, our and previous observations show that CH_4 in the upper estuary was unusually enriched in ^{13}C, sindicating that these isotopic signatures are likely inherited from riverine oxidation processes occurring upstream. Nevertheless, temporally

https://doi.org/10.5194/egusphere-2026-1582
Preprint. Discussion started: 26 March 2026

differential CH_4-isotope compositions suggests that seasonal variability strongly influences CH_4 production and oxidation dynamics.

Data availability. All data will be archived and made publicly available in the database DAS (Data Archive System, XXX).

Supplement. The supplement related to this article is available online at: XX.

Author contributions. The study was designed by AD, TR and HN. On-board sampling was performed by AD, DJBF, JK, DM and HN. Further geochemical analysis was conducted by AD, CV, SO and KB. Microbial rates were measured by AD and HN. Molecular analyses were performed by AD. HN supervised the research project. The paper was prepared by AD with input from all authors.

Acknowledgements. Our gratitude goes to the captain and crew of R/V Navicula as well as the staff of the geochemical, radioisotope and molecular laboratories at NIOZ (Sharyn Ossebaar, Maartje Brouwer, Judith van Bleijswijk Tierens Verhagen, Karel Bakker, Ronald van Bommel, Jort Ossebaar and Marcel van der Meer) and IMAU (Carina van der Veen), for their exceptional support. We would also like to extend our appreciation to Eric Wagemaakers for regularly calibrating the CTD. We acknowledge the Utrecht Sequencing Facility (USEQ) for providing sequencing service and data. USEQ is subsidized by the University Medical Center Utrecht and The Netherlands X-omics Initiative (NWO project 184.034.019).

https://doi.org/10.5194/egusphere-2026-1582
Preprint. Discussion started: 26 March 2026

Appendix A

Table A1. Water flow from Antwerp 100 m^3 s^{-1}, water flow to the North Sea 110 m^3 s^{-1}. With respect to individual measurements: F_{in} is 985 mol CH_4 d^{-1}, F_{out} is 674 mol CH_4 d^{-1}, J_{atm} is 1.4×10^6 mol CH_4 d^{-1}, MOx_{tot} is 1.7×10^4 mol CH_4 d^{-1}, MOg_{tot} is 1.4×10^6 mol CH_4 d^{-1}.

Station	km²	m³	CH_4 (nM)	MOx (nM d^{-1})	Efflux (mmol m^{-2} d^{-1})
10	4.94	31139580	114.0 ± 1.4	11.8 ± 0.2	3.4
9	7.12	29690140	101.4 ± 1.9	29.2 ± 0.7	1.5
8	8.33	85257713	52.2 ± 1.4	28.8 ± 0.9	0.9
7	16.33	169022630	57.6 ± 0.9	8.3 ± 0.1	5.5
6	17.82	179336603	56.3 ± 0	4.8 ± 0.3	2
5	31.94	248137846	60.3 ± 0.5	3.9 ± 0.1	2.4
4	43.58	435557352	91.6 ± 1.7	4.8 ± 0.2	6.3
3	60.80	658437303	184.1 ± 1.9	3.2 ± 0.2	12.7
2	24.47	417182404	140.5 ± 2.8	9.9 ± 1.5	4.7
1	36.83	432399513	70.9 ± 2.5	5.4 ± 0.4	0.2

https://doi.org/10.5194/egusphere-2026-1582
Preprint. Discussion started: 26 March 2026

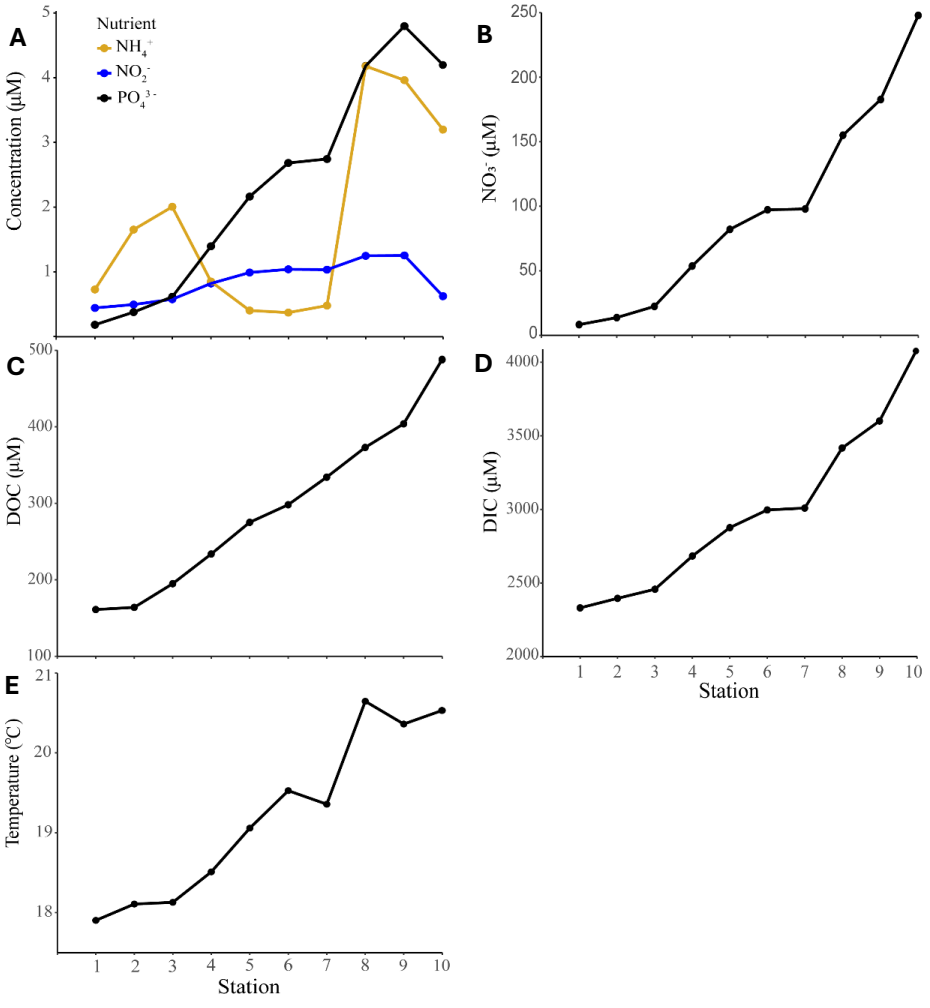

Figure A1. Properties of water column along the Scheldt Estuary**. A and B** Concentrations in µM of nutrients (NH_4^+, NO_2^-, PO_4^{3-} and NO_3^- **C and D** DOC and DIC in µM **E** Temperature.

https://doi.org/10.5194/egusphere-2026-1582
Preprint. Discussion started: 26 March 2026

References

Abdala Asbun, A., Besseling, M. A., Balzano, S., Van Bleijswijk, J. D., Witte, H. J., Villanueva, L., and Engelmann, J. C. Cascabel: a scalable and versatile amplicon sequence data analysis pipeline delivering reproducible and documented results. Frontiers in Genetics., 11, 489357, https://doi.org/10.3389/fgene.2020.489357, 2020.

Abril, G. and Iversen, N., Methane dynamics in a shallow, nontidal estuary (Randers Fjord, Denmark). Mar. Ecol. Prog. Ser. 230, 171–181, https://doi.org/10.3354/meps, 2002.

Abril, G., and Borges, A. V. Carbon dioxide and methane emissions from estuaries. In A. Tremblay, L. Varfalvy, C. Roehm, & M. Garneau (Eds.), Greenhouse gas emissions: fluxes and processes, hydroelectric reservoirs and natural environments., 187–207, https://doi.org/10.1007/3-540-26643-7_7, 2004.

Abril, G., Commarieu, M. V., & Guérin, F. Enhanced methane oxidation in an estuarine turbidity maximum. Limnology and oceanography, 52(1), 470-475, https://doi.org/10.4319/lo.2007.52.1.0470, 2007.

Borges, A. V., Champenois, W., Gypens, N., Delille, B., & Harlay, J. Massive marine methane emissions from near-shore shallow coastal areas. Scientific reports, 6(1), 27908, doi: 10.1038/srep27908, 2016.

Brass, M., and Röckmann, T.: Continuous-flow isotope ratio mass spectrometry method for carbon and hydrogen isotope measurements on atmospheric methane, Atmos. Meas. Tech., 3, 1707-1721, https://doi.org/10.5194/amt-3-1707-2010, 2010.

Brown, A. M., Bass, A. M., & Pickard, A. E. Anthropogenic-estuarine interactions cause disproportionate greenhouse gas production: A review of the evidence base. Marine Pollution Bulletin, 174, 113240, https://doi.org/10.1016/j.marpolbul.2021.113240, 2022.

Bussmann, I., Hackbusch, S., Schaal, P., and Wichels, A.: Data to: Methane concentration and oxidation in the Lena Delta, available at: https://doi.org/10.1594/PANGAEA.868494 (last access: November 2017), 2016.

Bussmann, I., Brix, H., Flöser, G., Ködel, U., & Fischer, P. Detailed patterns of methane distribution in the German Bight. Frontiers in Marine Science, 8, 728308, https://doi.org/10.3389/fmars.2021.728308, 2021.

Canadell, J. G., Monteiro, P. M. S., Costa, M. H., Cotrim da Cunha, L., Cox, P. M., Eliseev, A. V., Henson, S., Ishii, M., Jaccard, S., Koven, C., Lohila, A., Patra, P. K., Piao, S., Rogelj, J., Syampungani, S., Zaehle, S., and Zickfeld, K.: Global Carbon and other Biogeochemical Cycles and Feedbacks, in: Climate Change 2021: The Physical Science Basis. Contribution of Working Group I to the Sixth Assessment Report of the Intergovernmental Panel on Climate Change, edited by: Masson-Delmotte, V., Zhai, P., Pirani, A., Connors, S. L., Péan, C., Berger, S., Caud, N., Chen, Y., Goldfarb, L., Gomis, M. I., Huang, M., Leitzell, K., Lonnoy, E., Matthews, J. B. R., Maycock, T. K., Waterfield, T., Yelekçi, O., Yu, R., and Zhou, B., Cambridge University Press, 673–816, https://doi.org/10.1017/9781009157896.007, 2021.

Canning, A., Wehrli, B., & Körtzinger, A. Methane in the Danube Delta: the importance of spatial patterns and diel cycles for atmospheric emission estimates. Biogeosciences, 18(12), 3961-3979, https://doi.org/10.5194/bg-18-3961-2021, 2021.

Ciais, P., Sabine, C., Bala, G., Bopp, L., Brovkin, V., Canadell, J., Chhabra, A., DeFries, R., Galloway, J., Heimann. M, Jones, C., Le Quéré, C., Myneni, R. B., Piao, S., and Thornton, P.: Carbon and Other Biogeochemical Cycles, in In Climate Change 2013: The Physical Science Basis. Contribution of Working Group I to the Fifth Assessment Report of IPCC, edited by: Stocker, T. F., Qin, D., Plattner, G.-K., Tignor, M., Allen, S. K., Boschung, J., Nauels, A., Xia, Y., Bex, V., and Midgley, P. M., Cambridge University Press, Cambridge, ISBN 978-1-107-05799-1, 2013.

https://doi.org/10.5194/egusphere-2026-1582
Preprint. Discussion started: 26 March 2026

Das, B. K., Chakraborty, H. J., Kumar, V., Rout, A. K., Patra, B., Das, S. K., & Behera, B. K. Comparative metagenomic analysis from Sundarbans ecosystems advances our understanding of microbial communities and their functional roles. Scientific Reports, 14(1), 16218, https://doi.org/10.1038/s41598-024-67240-1, 2024.

de Angelis, M. A. and Scranton, M. I. Fate of methane in the Hudson River and estuary. Global Biogeochemical Cycles, 7(3), 509-523, https://doi.org/10.1029/93GB01636, 1993.

de Groot, T.R., Mol, A.M., Mesdag, K., Ramond, P., Ndhlovu, R., Engelmann, J.C., Röckmann, T. and Niemann, H., Diel and seasonal methane dynamics in the shallow and turbulent Wadden Sea. Biogeosciences, 20(18), pp.3857-3872., https://doi.org/10.5194/bg-20-3857-2023, 2023.

de Groot, T.R., Menoud, M., van Bleijswijk, J., van Leeuwen, S.M., van der Molen, J., Hernando-Morales, V., Czerski, H., Maazallahi, H., Walter, S., Rush, D. and Röckmann, T., Tidal and seasonal influence on cold seep activity and methanotroph efficiency in the North Sea. Communications Earth & Environment, 5(1), p.368, https://doi.org/10.25850/nioz/7b.b.jh, 2024.

de Groot, T. R., Engelmann, J. C., Ramond, P., Diorgio, J., van Bleiswijk, J., & Niemann, H., Adaptation of methane oxidising bacteria to environmental changes: implications for coastal methane dynamics. EGUsphere, 1-21, https://doi.org/10.5194/egusphere-2025-316, 2025.

von Deimling, J.S., Rehder, G., Greinert, J., McGinnnis, D.F., Boetius, A. and Linke, P., Quantification of seep-related methane gas emissions at Tommeliten, North Sea. Continental Shelf Research, 31(7-8), pp.867-878, https://doi.org/10.1016/j.csr.2011.02.012, 2011.

Delre, A., Goudriaan, M., Morales, V.H., Vaksmaa, A., Ndhlovu, R.T., Baas, M., Keijzer, E., de Groot, T., Zeghal, E., Egger, M. and Röckmann, T., Plastic photodegradation under simulated marine conditions. Marine Pollution Bulletin, 187, p.114544, https://doi.org/10.1016/j.marpolbul.2022.114544, 2023.

Dumestre, J. F., Guézennec, J., Galy-Lacaux, C., Delmas, R., Richard, S., & Labroue, L. Influence of light intensity on methanotrophic bacterial activity in Petit Saut Reservoir, French Guiana. Applied and environmental microbiology, 65(2), 534-539, https://doi.org/10.1128/AEM.65.2.534-539.1999,1999.

Etminan, M., Myhre, G., Highwood, E. J., and Shine, K. P.: Radiative forcing of carbon dioxide, methane, and nitrous oxide: A significant revision of the methane radiative forcing, Geophys. Res. Lett., 43, 12614–12623, https://doi.org/10.1002/2016gl071930, 2016.

Ferrón, S., Ortega, T., Gómez-Parra, A., Forja, J.M.,. Seasonal study of dissolved CH4, CO2 and N in a shallow tidal system of the Bay of Cádiz (SW Spain). J. Mar. Syst. 66, 244–257, https://doi.org/10.1016/j.jmarsys.2006.03.021, 2007.

Fluet-Chouinard, E., Stocker, B.D., Zhang, Z., Malhotra, A., Melton, J.R., Poulter, B., Kaplan, J.O., Goldewijk, K.K., Siebert, S., Minayeva, T. and Hugelius, G.. Extensive global wetland loss over the past three centuries. Nature, 614(7947), pp.281-286, https://doi.org/10.5281/zenodo.7293597,2023.

Gentz, T., Damm, E., von Deimling, J. S., Mau, S., McGinnis, D. F., & Schlüter, M. A water column study of methane around gas flares located at the West Spitsbergen continental margin. Continental Shelf Research, 72, 107-118, https://doi.org/10.1016/j.csr.2013.07.013, 2014.

Grasshoff, P., Methods of seawater analysis. Verlag Chemie. FRG, 419, pp.61-72,1983.

Green, J. D.: Headspace analysis Static, in: Encyclopedia of Analytical Science (Second Edition), edited by: Worsfold, P., Townshend, A., and Poole, C., Elsevier, Oxford, 229–236, https://doi.org/10.1016/B0-12-369397-7/00254-5, 2005.

https://doi.org/10.5194/egusphere-2026-1582
Preprint. Discussion started: 26 March 2026

Groffen, T., Schoutens, K., Zamora, J. D., Gourgue, O., Bervoets, L., & Temmerman, S. (2025). Spatial distribution of per-and polyfluoroalkyl substances (PFAS) in natural and restored intertidal wetlands in the Scheldt estuary. Journal of Hazardous Materials, 139247.

Gropp, J., Jin, Q. & Halevy, I. Controls on the isotopic composition of microbial methane. Sci. Adv. **8**, eabm5713 (2022).

Guérin, F., & Abril, G. (2007). Significance of pelagic aerobic methane oxidation in the methane and carbon budget of a tropical reservoir. Journal of Geophysical Research: Biogeosciences, 112(G3).

Hackbusch, S., Wichels, A., & Bussmann, I. (2019). Abundance, activity and diversity of methanotrophic bacteria in the Elbe Estuary and southern North Sea. Aquatic microbial ecology, 83(1), 35-48.

Helder, W., & De Vries, R. T. P. (1979). An automatic phenol-hypochlorite method for the determination of ammonia in sea-and brackish waters. Netherlands Journal of Sea Research, 13(1), 154-160.

Hirayama, H., Fuse, H., Abe, M., Miyazaki, M., Nakamura, T., Nunoura, T., Furushima, Y., Yamamoto, H., and Takai, K.: Methylomarinum vadi gen. nov., sp. nov., a methanotroph isolated from two distinct marine environments, Int. J. Syst. Evol. Microb., 63, 1073–1082, https://doi.org/10.1099/ijs.0.040568-0, 2013.

Ho, A., Mo, Y., Lee, H. J., Sauheitl, L., Jia, Z., and Horn, M. A.: Effect of salt stress on aerobic methane oxidation and associated methanotrophs; a microcosm study of a natural community from a non-saline environment, Soil Biol. Biochem., 125, 210–214, https://doi.org/10.1016/j.soilbio.2018.07.013, 2018.

Jacques, C., Gkritzalis, T., Tison, J.-L., Hartley, T., van der Veen, C., Röckmann, T., Middelburg, J. J., Cattrijsse, A., Egger, M., Dehairs, F., and Sapart, C. J.: Carbon and Hydrogen Isotope Signatures of Dissolved Methane in the Scheldt Estuary, Estuar. Coasts, 44, 137–146, https://doi.org/10.1007/s12237-020-00768-3, 2021.

Jakobs, G., Rehder, G., Jost, G., Kießlich, K., Labrenz, M., & Schmale, O. (2013). Comparative studies of pelagic microbial methane oxidation within the redox zones of the Gotland Deep and Landsort Deep (central Baltic Sea). Biogeosciences, 10(12), 7863-7875.

James, R. H., Bousquet, P., Bussmann, I., Haeckel, M., Kipfer, R., Leifer, I., Niemann, H., Ostrovsky, I., Piskozub, J., Rehder, G., Treude, T., Vielstädte, L., and Greinert, J.: Effects of climate change on methane emissions from seafloor sediments in the Arctic Ocean: A review, Limnol. Oceanogr., 61, 283–299, https://doi.org/10.1002/lno.10307, 2016.

Jordan, S. F. A., Treude, T., Leifer, I., Janssen, R., Werner, J., Schulz-Vogt, H., and Schmale, O.: Bubble-mediated transport of benthic microorganisms into the water column: Identification of methanotrophs and implication of seepage intensity on transport efficiency, Sci. Rep., 10, 4682, https://doi.org/10.1038/s41598-020-61446-9, 2020.

Jordan, S. F. A., Gräwe, U., Treude, T., van der Lee, E. M., Schneider von Deimling, J., Rehder, G., and Schmale, O.: Pelagic Methane Sink Enhanced by Benthic Methanotrophs Ejected From a Gas Seep, Geophys. Res. Lett., 48, e2021GL094819, https://doi.org/10.1029/2021GL094819, 2021.

Kelley, C.A., Martens, C.S., Chanton, J.P., Variations in sedimentary carbon remineralization rates in the White Oak River estuary, North Carolina. Limnology and Oceanography 35, 372–38, https://doi.org/10.4319/lo.1990.35.2.0372, 1990.

Kitidis, V., Tizzard, L., Uher, G., Judd, A., Upstill-Goddard, R.C., Head, I.M., Gray, N.D., Taylor, G., Durán, R., Diez, R., Iglesias, J., García-Gil, S., The biogeochemical cycling of methane in ria De Vigo, NW Spain: sediment processing and sea–air exchange. J. Mar. Syst. 66, 258–271, https://doi.org/10.1016/j.jmarsys.2006.03.022, 2007.

https://doi.org/10.5194/egusphere-2026-1582
Preprint. Discussion started: 26 March 2026

Klappenbach, J. A., Saxman, P. R., Cole, J. R., & Schmidt, T. M. rrndb: the ribosomal RNA operon copy number database. Nucleic acids research, 29(1), 181-184, https://doi.org/10.1093/nar/29.1.181, 2001.

Knief, C.: Diversity and Habitat Preferences of Cultivated and Uncultivated Aerobic Methanotrophic Bacteria Evaluated Based on pmoA as Molecular Marker, Front. Microb., 6, 1346, https://doi.org/10.3389/fmicb.2015.01346, 2015.

Krzycki, J. A., Kenealy, W. R., DeNiro, M. J. & Zeikus, J. G. Stable Carbon Isotope Fractionation by Methanosarcina barkeri during Methanogenesis from Acetate, Methanol, or Carbon Dioxide-Hydrogen. Appl. Environ. Microbiol. **53**, 2597–2599, https://doi.org/10.1128/aem.53.10.2597-2599.1987, 1987.

Lan, X., Thoning, K. W., and Dlugokencky, E. J.: Trends in globally-averaged CH_4, N_2O, and SF6 determined from NOAA Global Monitoring Laboratory measurements Version 2024-02, Global Monitoring Laboratory [data set], https://doi.org/10.15138/P8XG-AA10, 2024.

Legg, S., IPCC, 2021: Climate change 2021-the physical science basis. *Interaction*, *49*(4), pp.44-45, 2021.

Leifer, I. and Patro, R. K. The bubble mechanism for methane transport from the shallow sea bed to the surface: a review and sensitivity study. Cont. Shelf Res. 22, 2409–2428, https://doi.org/10.1016/S0278-4343(02)00065-1,2002.

Lofton, D., Whalen, S., and Hershey, A.: Effect of temperature on methane dynamics and evaluation of methane oxidation kinetics in shallow Arctic Alaskan lakes, Hydrobiologia, 721, 209–222, https://doi.org/10.1007/s10750-013-1663-x, 2014.

Mayr, M. J., Zimmermann, M., Dey, J., Brand, A., Wehrli, B., & Bürgmann, H. Growth and rapid succession of methanotrophs effectively limit methane release during lake overturn. *Communications biology*, *3*(1), 108, https://doi.org/10.1038/s42003-020-0838-z, 2020.

Mao, S.-H., Zhang, H.-H., Zhuang, G.-C., Li, X.-J., Liu, Q., Zhou, Z., Wang, W.-L., Li, C.-Y., Lu, K.-Y., Liu, X.-T., Montgomery, A., Joye, S. B., Zhang, Y.-Z., & Yang, G.-P. Aerobic oxidation of methane significantly reduces global diffusive methane emissions from shallow marine waters. Nature Communications, 13, 7309. https://doi.org/10.1038/s41467-022-35082-y, 2022.

Matoušů, A., Osudar, R., Šimek, K., & Bussmann, I. Methane distribution and methane oxidation in the water column of the Elbe estuary, Germany. Aquatic Sciences, 79(3), 443-458, https://doi.org/10.1007/s00027-016-0509-9, 2017.

Mau, S., Blees, J., Helmke, E., Niemann, H., and Damm, E.: Vertical distribution of methane oxidation and methanotrophic response to elevated methane concentrations in stratified waters of the Arctic fjord Storfjorden (Svalbard, Norway), Biogeosciences, 10, 6267–6278, https://doi.org/10.5194/bg-10-6267-2013, 2013.

McGinnis, D. F., Greinert, J., Artemov, Y., Beaubien, S. E. & Wuest, A. Fate of rising methane bubbles in stratified waters: How much methane reaches the atmosphere ? J. Geophys. Res. 111, 1–15, https://doi.org/10.1029/2005JC003183 , 2006.

Meire, P., Ysebaert, T., Damme, S. V., Bergh, E. V. D., Maris, T., & Struyf, E. (2005). The Scheldt estuary: a description of a changing ecosystem. Hydrobiologia, 540, 1-11, https://doi.org/10.1007/s10750-005-0896-8, 2005.

Middelburg, J. J., Nieuwenhuize, J., Iversen, N., Høgh, N., de Wilde, H., Helder, W., Seifert, R., and Christof, O.: Methane distribution in European tidal estuaries, Biogeochemistry, 59, 95–119, https://doi.org/10.1023/A:1015515130419, 2002.

https://doi.org/10.5194/egusphere-2026-1582
Preprint. Discussion started: 26 March 2026

Murase, J., and Sugimoto, A. Inhibitory effect of light on methane oxidation in the pelagic water column of a mesotrophic lake (Lake Biwa, Japan). Limnology and oceanography, 50(4), 1339-1343, https://doi.org/10.4319/lo.2005.50.4.1339, 2005.

Murphy, J. and Riley, J.P., A modified single solution method for the determination of phosphate in natural waters. Analytica chim. Acta, 27, p31-36, 1962

Niemann, H., Steinle, L., Blees, J., Bussmann, I., Treude, T., Krause, S., Elvert, M., and Lehmann, M. F.: Toxic effects of lab-grade butyl rubber stoppers on aerobic methane oxidation, Limnol. Oceanogr.-Meth., 13, 40–52, https://doi.org/10.1002/lom3.10005, https://doi.org/10.1016/S0003-2670(00)88444-5, 2015.

Osudar, R., Matoušů, A., Alawi, M., Wagner, D., and Bussmann, I.: Environmental factors affecting methane distribution and bacterial methane oxidation in the German Bight (North Sea), Estuar. Coast. Shelf Sci., 160, 10–21, https://doi.org/10.1016/j.ecss.2015.03.028, 2015.

Osudar, R., Klings, K. W., Wagner, D., and Bussmann, I.: Effect of salinity on microbial methane oxidation in freshwater and marine environments, Aquat. Microb. Ecol., 80, 181–192, https://doi.org/10.3354/ame01845, 2017.

Parnell, A. C., Inger, R., Bearhop, S., & Jackson, A. L. Source partitioning using stable isotopes: coping with too much variation. PloS one, 5(3), e9672, https://doi.org/10.1371/journal.pone.0009672, 2010.

Perrot, V., Ma, T., Vandeputte, D., Smolikova, V., Bratkic, A., Leermakers, M., Baeyens, W. and Gao, Y., Origin and partitioning of mercury in the polluted Scheldt Estuary and adjacent coastal zone. Science of the Total Environment, 878, p.163019, https://doi.org/10.1016/j.scitotenv.2023.163019, 2023.

Poffenbarger, H. J., Needelman, B. A., & Megonigal, J. P. Salinity influence on methane emissions from tidal marshes. Wetlands, 31(5), 831-842, https://doi.org/10.1007/s13157-011-0197-0, 2011.

Quast, C., Pruesse, E., Yilmaz, P., Gerken, J., Schweer, T., Yarza, P., Peplies, J. and Glöckner, F.O., The SILVA ribosomal RNA gene database project: improved data processing and web-based tools. Nucleic acids research, 41(D1), pp.D590-D596, https://doi.org/10.1093/nar/gks1219, 2012.

Reeburgh, W. S.: Oceanic Methane Biogeochemistry, Chem. Rev., 107, 486–513, https://doi.org/10.1021/cr050362v, 2007.

Rehder, G., Keir, R. S., Suess, E., and Pohlmann, T. The Multiple Sources and Patterns of Methane in North Sea Waters. Aquatic Geochemistry, 4(3), 403-427, https://doi.org/10.1023/A:1009644600833, 1998.

Röckmann, T., Eyer, S., van der Veen, C., Popa, M. E., Tuzson, B., Monteil, G., Houweling, S., Harris, E., Brunner, D., Fischer, H., Zazzeri, G., Lowry, D., Nisbet, E. G., Brand, W. A., Necki, J. M., Emmenegger, L., and Mohn, J.: In situ observations of the isotopic composition of methane at the Cabauw tall tower site, Atmos. Chem. Phys., 16, 10469–10487, https://doi.org/10.5194/acp-16-10469-2016, 2016.

Rosentreter, J. A., Laruelle, G. G., Bange, H. W., Bianchi, T. S., Busecke, J. J. M., Cai, W.-J., Eyre, B. D., Forbrich, I., Kwon, E. Y., Mavara, T., Moosdorf, N., Van Dam, B., and Regnier, P.: Coastal vegetation and estuaries are collectively a greenhouse gas sink, Nat. Clim. Change, 13, 579–587, https://doi.org/10.1038/s41558-023-01682-9, 2023.

Sánchez-Rodríguez, J., Sierra, A., Jiménez-López, D., Ortega, T., Gómez-Parra, A., & Forja, J. Dynamic of CO2, CH4 and N2O in the Guadalquivir estuary. Science of The Total Environment, 805, 150193, https://doi.org/10.1016/j.scitotenv.2021.150193, 2022.

https://doi.org/10.5194/egusphere-2026-1582
Preprint. Discussion started: 26 March 2026

Sasakawa, M., Tsunogai, U., Kameyama, S., Nakagawa, F., Nojiri, Y., & Tsuda, A. Carbon isotopic characterization for the origin of excess methane in subsurface seawater. Journal of Geophysical Research: Oceans, 113(3). https://doi.org/10.1029/2007JC004217, 2008.

Schmale, O., Leifer, I., Deimling, J. S. v., Stolle, C., Krause, S., Kießlich, K., Frahm, A., and Treude, T.: Bubble Transport Mechanism: Indications for a gas bubble-mediated inoculation of benthic methanotrophs into the water column, Cont. Shelf Res., 103, 70–78, https://doi.org/10.1016/j.csr.2015.04.022, 2015.

Scranton, M.I., and K. McShane. 1991. Methane fluxes in the southern North Sea: the role of European rivers. Continental Shelf Research 11 (1): 37–52. https://doi.org/10.1016/0278-4343(91)90033-3.

Sherry, A., Osborne, K. A., Sidgwick, F. R., Gray, N. D., & Talbot, H. M. A temperate river estuary is a sink for methanotrophs adapted to extremes of pH, temperature and salinity. Environmental Microbiology Reports, 8(1), 122-131, https://doi.org/10.1111/1758-2229.12359, 2016.

Silvennoinen, H., Liikanen, A., Rintala, J., Martikainen, P.J., Greenhouse gas fluxes from the eutrophic Temmesjoki River and its estuary in the Liminganlahti Bay (the Baltic Sea). Biogeochemistry 90, 193–208, https://doi.org/10.1007/s10533-008-9244-1, 2008.

Soetaert, K., Middelburg, J. J., Heip, C. H. R., Meire, P., Van Damme, S., & Maris, T. (2006). Long-term change in dissolved inorganic nutrients in the heterotrophic Scheldt estuary (Belgium, the Netherlands). Limnology and Oceanography, 51(1), 409 423. https://doi.org/10.4319/lo.2006.51.1_part_2.0409

Stanley, E. H., Loken, L. C., Casson, N. J., Oliver, S. K., Sponseller, R. A., Wallin, M. B., ... & Rocher-Ros, G. GRiMeDB: The global river database of methane concentrations and fluxes. Earth System Science Data Discussions, 2022, 1-94, https://doi.org/10.6073/pasta/b7d1fba4f9a3e365c9861ac3b58b4a90 , 2022.

Steinle, L., Graves, A. C., Treude, T., Ferré, B., Biastoch, A., Bussmann, I., Berndt, C., Krastel, S., James, R. H., Behrens, E., Böning, C. W., Greinert, J., Sapart, C., Scheinert, M., Sommer, S., Lehmann, M. F., and Niemann, H.: Water column methanotrophy controlled by a rapid oceanographic switch, Nat. Geosci., 8, 378–382, https://doi.org/10.1038/ngeo2420, 2015.

Stoll, M.H.C, Bakker K., Nobbe G.H., Haese R.R., Analytical Chemistry, Vol 73, Number 17, pp 4111-4116, https://doi.org/10.1021/ac010303r, 2001.

Struyf, E., Van Damme, S., & Meire, P. Possible effects of climate change on estuarine nutrient fluxes: a case study in the highly nutrified Schelde estuary (Belgium, The Netherlands). Estuarine, Coastal and Shelf Science, 60(4), 649-661, https://doi.org/10.1016/j.ecss.2004.03.004, 2004.

Tavormina P. L., Ussler W. III, Orphan V. J. Planktonic and sediment-associated aerobic methanotrophs in two seep systems along the North American margin. Appl Environ Microbiol, https://doi.org/10.1128/AEM.00069-08, 2008.

Tavormina, P. L., Hatzenpichler, R., McGlynn, S., Chadwick, G., Dawson, K. S., Connon, S. A., and Orphan, V. J.: Methyloprofundus sedimenti gen. nov., sp. nov., an obligate methanotroph from ocean sediment belonging to the "deep sea-1" clade of marine methanotrophs, Int. J. Syst. Evol. Microb., 65, 251–259, https://doi.org/10.1099/ijs.0.062927-0, 2015.

Upstill-Goddard, R. C., and Barnes, J. Methane emissions from UK estuaries: re-evaluating the estuarine source of tropospheric methane from Europe. Marine Chemistry, 180, 14-23, https://doi.org/10.1016/j.marchem.2016.01.010, 2016.

https://doi.org/10.5194/egusphere-2026-1582
Preprint. Discussion started: 26 March 2026

Van Ael, E., Covaci, A., Blust, R., and Bervoets, L. Persistent organic pollutants in the Scheldt estuary: environmental distribution and bioaccumulation. Environment international, 48, 17-27, https://doi.org/10.1016/j.envint.2012.06.017, 2012.

Van Damme, S., Struyf, E., Maris, T., Ysebaert, T., Dehairs, F., Tackx, M., Heip, C. H. R., & Meire, P. Spatial and temporal patterns of water quality along the estuarine salinity gradient of the Scheldt estuary (Belgium and the Netherlands): Results of an integrated monitoring approach. Hydrobiologia, 540, 29 - 45, https://doi.org/10.1007/s10750-004-7102-2, 2005.

Vekeman, B., Kerckhof, F.M., Cremers, G., De Vos, P., Vandamme, P., Boon, N., Op den Camp, H.J. and Heylen, K., 2016. New Methyloceanibacter diversity from North Sea sediments includes methanotroph containing solely the soluble methane monooxygenase. Environmental microbiology, 18(12), pp.4523-4536, https://doi.org/10.1111/1462-2920.13485, 2016.

Whiticar, M. J.: Carbon and hydrogen isotope systematics of bacterial formation and oxidation of methane, Chem. Geol., 161, 291–314, https://doi.org/10.1016/S0009-2541(99)00092-3, 1999.

Wiesenberg, D. A. and Guinasso, N. L.: Equilibrium Solubilities of Methane, Carbon Monoxide, and Hydrogen in Water and Sea Water, J. Chem. Eng. Data, 24, 356–360, https://doi.org/10.1021/je60083a006, 1979.

Woodward, G., Perkins, D. M., and Brown, L. E.: Climate change and freshwater ecosystems: impacts across multiple levels of organization, Philos T. R. Soc. Lond. B, 365, 2093–2106, https://doi.org/10.1098/rstb.2010.0055, 2010.

Wu, Z., Li, M., Qu, L., Zhang, C. and Xie, W. Metagenomic insights into microbial adaptation to the salinity gradient of a typical short residence-time estuary. Microbiome 12, 115, https://doi.org/10.1186/s40168-024-01817-w, 2024.

Yang, Y., Chen, J., Pratscher, J., and Xie, S. DNA-SIP reveals an overlooked methanotroph, Crenothrix sp., involved in methane consumption in shallow lake sediments. Science of the Total Environment, 814, 152742, https://doi.org/10.1016/j.scitotenv.2021.152742, 2022.

Zhang, G., Zhang, J., Lui, S., Ren, J., Xu, J., Zhang, F., Methane in the Changjiang (Yangtze River) Estuary and its adjacent marine area: riverine input, sediment release and atmospheric fluxes. Biogeochemistry 91, 71–84, https://doi.org/10.1007/s10533-008-9259-7, 2008.

Zhang, S., Yan, L., Cao, J., Wang, K., Luo, Y., Hu, H., Wang, L., Yu, R., Pan, B., Yu, K., Zhao, J., and Bao, Z.: Salinity significantly affects methane oxidation and methanotrophic community in Inner Mongolia lake sediments, Front. Microbiol., 13, 1067017, https://doi.org/10.3389/fmicb.2022.1067017, 2023.